



AN ANALYTICAL MODEL FOR RC COLUMNS SUBJECTED TO COMBINED LOADINGS INCLUDING TORSION

Y.M. You¹ and A. Belarbi²

¹ Post-Doctoral Fellow, Department of Civil, Environmental and Architectural Engineering,
Missouri S & T, Rolla, Missouri, USA.

² Distinguished Professor, Department of Civil, Environmental and Architectural Engineering,
Missouri S & T, Rolla, Missouri, USA.

Email : ¹youngmin@mst.edu, ²belarbi@mst.edu

ABSTRACT :

Reinforced concrete (RC) columns can be subjected to torsional moments in addition to flexural, axial and shear forces during earthquake excitations. Therefore, it is essential to develop models to predict their behavior under combined loadings. The objective of this study is to propose a rational model capable of predicting the entire loading history of circular RC columns under combined loading. As an initial step of this study, an analytical model for RC columns subjected to torsion and axial force is developed. The existing rotating-angle softened truss model (RA-STM) was chosen as a basis and it was modified to account for tension-stiffening effect and biaxial constitutive laws of R C in the proposed model. This addition makes it possible to estimate the thickness of shear flow zone. As a result, it is possible to predict the torque-twist curve of circular RC column even after the post-peak behavior. The performance of proposed method is validated with the test results of a half-scale circular RC column under torsion and axial compression. The proposed model can be used as a basis to predict the behavior of circular RC columns under combined loadings including shear and flexure.

KEYWORDS: softened truss model, circular column, torsion, shear flow zone, combined loading

1. INTRODUCTION

The behavior of a reinforced concrete (RC) member under shear and torsion can be predicted by the three most well-known truss models, the modified compression field theory (MCFT) (Vecchio and Collins 1986), the rotating-angle softened truss model (RA-STM) (Hsu 1988), the fixed-angle softened truss model (FA-STM) (Pang and Hsu 1996; Hsu and Zhang 1997). These theories commonly assume RC member as assemblies of two-dimensional membrane elements, also called panels, subjected to in-plane shear and normal stresses. Therefore, the behavior of a RC member under shear and torsion can be predicted via the behavior of membrane elements. The most critical issue in assembling the membrane elements to a torsional RC member is in proper estimation of the thickness of shear flow zone, t_d , during the load-deformation response. The estimation of t_d in a torsional rectangular member is relatively well established than in a non-rectangular section member, especially in a member like bridge column with circular cross section. Although there is a considerable debate over the estimation of t_d in STM and MCFT with respect to spalling effect, they both tend to agree that t_d in a torsional rectangular member is strongly affected by out-of-plane warping, which causes bending in the concrete struts. Also, there is no established theory for the out-of-plane warping effect in a torsional circular member. However, it is physically apparent that out-of-plane warping effect on a circular section member is considerably smaller than that on a rectangular section member. In other words, the concrete struts in a torsional circular member are predominated by the in-plane principal compression and tension due to the circulatory shear. In spite of this apparent physical phenomenon, most of design codes or specifications adopt the similar concept of a torsional rectangular member suggested by STM and MCFT when estimating t_d in a torsional circular member at the ultimate state. Thus, this discrepancy should be amended based on a basic physical phenomenon in a torsional circular section. Although many aspects of MCFT and STM are similar, their treatment of the shear flow zone and the stress-strain relationship for concrete in

compression differ significantly. To predict the overall behavior of a torsional circular member including the spalling effect, the STM is a more suitable model than the MCFT not only in the case of the proper estimation of t_d , but also in other mechanical aspects (Hsu 1998). The softening truss model (STM) proposed by Hsu (Hsu 1985), which was based on the rotating angle concept, has improved remarkably during last two decades on two main streams. One is in improvement of material laws for concrete and steel (Belarbi and Hsu 1994, 1995; Hsu and Zhang 1996; Hsu and Zhu 2001), and the other is in improvement of STM itself (Pang and Hsu 1996; Hsu and Zhang 1997; Greene 2006).

Although there have been significant improvement of truss models themselves, all of these models have difficulties predicting the post-peak behavior which is very important in the seismic design. This is caused due to the neglect of Poisson effect in RC elements under biaxial stress field. In other words, material laws for concrete and steel used in truss models should be derived from the biaxial stress and strain conditions. However, all the models developed so far have adopted the material laws derived from uniaxial conditions. Sengupta and Belarbi (2001) studied this problem by the estimation of proper Poisson's ratios by testing 18 panels under biaxial loading. However, they could not define the Poisson's ratios accurately due to the limitation of testing facility. More sophisticated experimental investigation about the Poisson effect in RC membrane elements was carried out by Hsu and Zhu (2002) using a unique panel testing facility. They finally suggested the Hsu/Zhu ratios through test results of twelve full-size RC panels considering four variables and developed a new model called softened-membrane-model (SMM), which can predict the entire behavioral history including both the pre-peak and post-peak behavior. For this study, RA-STM is chosen as a proper model to analyze the RC circular columns under torsion and axial force. A generalized algorithm incorporating the proper estimation of t_d , the tension stiffening effect and Poisson effect is introduced and validated by comparing with test results. This paper presents a rational and general method based on RA-STM to analyze the entire behavior of a circular RC column under pure torsion with or without axial compression from existing experimental results. Particularly, exact value of t_d can be calculated through the proposed algorithm and will be a valuable piece of information for understanding the mechanical behavior of circular RC member under pure torsion. Moreover, this method can also be applicable to a rectangular RC member under pure torsion. This flexibility makes it possible to use the proposed algorithm as a verification tool for both experimental and analytical results of RC members with any cross section under pure torsion.

2. GOVERNING EQUATIONS AND MODIFICATIONS OF RA-STM

2.1 Governing Equations

When applying the RA-STM to a rectangular section subjected to a torque, all the following equations satisfies Navier's principle, which comprise of four equilibrium equations, seven compatibility equations, and five constitutive laws for concrete and steel. These equations are given in a paper by Hsu (1988) with all pertaining figures and are not repeated here due to space limitation. In the original RA-STM, concrete tensile stress, σ_r , is considered as zero. This assumption results in significant overestimation of deformation due to the neglect of tension stiffening effect. The effect of tension stiffening can be taken into account by incorporating the average tensile stress-strain relationship of concrete in the analysis.

2.1.1 Equilibrium equations

The two-dimensional equilibrium condition relates the average internal stresses in the concrete (σ_d and σ_r) and in the reinforcement (f_l and f_t) to the average applied stresses (σ_l , σ_t and τ_{lt}) with respect to the angle of inclination of the d-axis to the l-axis (α).

$$\sigma_l = \sigma_d \cos^2 \alpha + \sigma_r \sin^2 \alpha + \rho_l f_l \quad (2.1)$$

$$\sigma_t = \sigma_d \sin^2 \alpha + \sigma_r \cos^2 \alpha + \rho_t f_t \quad (2.2)$$

$$\tau_{lt} = (-\sigma_d + \sigma_r) \sin \alpha \cos \alpha \quad (2.3)$$

$$T = \tau_{lt} (2A_0 t_d) \quad (2.4)$$

2.1.2 Compatibility equations

The 2-D compatibility condition expresses the relationship between the average strains in different coordinate systems, namely: the l - t -coordinate system ($\varepsilon_l, \varepsilon_t$ and γ_{lt}) and the d - r principal axes ($\varepsilon_d, \varepsilon_r$). Additional equations are needed to solve the torsional problem accounting for the strain and stress distributions in concrete struts affected by the out-of-plane warping effects. The curvature of the concrete struts (ψ) can be related by geometry to the angle of twist (θ), α , the thickness of shear flow zone (t_d) and the outer face strain of the concrete strut (ε_{ds}).

$$\varepsilon_l = \varepsilon_d \cos^2 \alpha + \varepsilon_r \sin^2 \alpha \quad (2.5)$$

$$\varepsilon_t = \varepsilon_d \sin^2 \alpha + \varepsilon_r \cos^2 \alpha \quad (2.6)$$

$$\frac{\gamma_{lt}}{2} = (-\varepsilon_d + \varepsilon_r) \sin \alpha \cos \alpha \quad (2.7)$$

$$\theta = \frac{P_0}{2A_0} \gamma_{lt} \quad (2.8)$$

$$\psi = \theta \sin 2\alpha \quad (2.9)$$

$$t_d = \varepsilon_{ds} / \psi \quad (2.10)$$

$$\varepsilon_d = \varepsilon_{ds} / 2 \quad (2.11)$$

2.1.3 Constitutive laws

$$\sigma_d = k_1 \zeta f'_c \Rightarrow f(\varepsilon_d, \zeta) \quad (2.12)$$

$$k_1 = f(\varepsilon_{ds}, \zeta) \quad (2.13)$$

$$\zeta = f(\varepsilon_d, \varepsilon_r) \quad (2.14)$$

$$f_l = f(\varepsilon_l) \quad (2.15)$$

$$f_t = f(\varepsilon_t) \quad (2.16)$$

$$\sigma_r = 0 \Rightarrow f_r(\varepsilon_r) \quad (2.17)$$

Table 2.1 List of equations and variables in the proposed method

Category	Variables			Equations		
	Stresses or force	Strains Or Geometry	Material	Equilibrium	Compatibility	Material (Constitutive)
For Shear	σ_l	ε_l	ζ	(2.1)	(2.5)	(2.14)
	σ_t	ε_t		(2.2)	(2.6)	
	τ_{lt}	γ_{lt}		(2.3)	(2.7)	
	σ_d	ε_d				(2.12)
	σ_r	ε_r				(2.17)
	f_l	α				(2.15)
	f_t					(2.16)
Additional For torsion	T	θ	(k_1)	(2.4)	(2.8)	(2.13)
		(ψ)			(2.9)	
		t_d			(2.10)	
		(ε_{ds})			(2.11)	
Number	8(7)	8(10)	1(2)	4(4)	4(7)	5(5)
Total		17(19)			13(16)	

* $\sigma_l = \sigma_t = 0$ (pure torsion), $\sigma_l = c$ (with axial force)

2.2 Variables and Equations

All the variables and equations related to out-of-plane warping effect on flat concrete wall causing bending in concrete struts are eliminated from the original RA-STM method in order to remove the ambiguous estimation of t_d in a circular shaped concrete wall as shown in Table 2.1. That is, equations related with Bredt's theory which are Eqn. (2.4) and (2.8) are only considered in the proposed method. The elimination of variables and equations increases the number of unknowns between the equations and variables and makes them unbalance. Therefore, it is necessary to resolve this problem by introducing new variables and equations. Thus, the terms related with concrete properties in tension are augmented in the proposed method not only to resolve the unbalance between the number of equations and variables but also to consider the tension stiffening effect. From the mechanical point of view, this is a reasonable assumption only if Navier's principle is satisfied. As a result, the number of unknown variables reduced from 19 to 17, and the number of governing equations also reduced from 16 to 13. That is, the number of differences between unknown variables and governing equations increases by one more. In the original RA-STM method, these discrepancies between unknown variables and equations were iteratively resolved by taking apparent two constant values, $\sigma_l = \sigma_r = 0$, and an arbitrary constant, ε_d , for three unknown variables as shown in Table 2.2. Adjustment on differences in the proposed method is achieved from two apparent variables, $\sigma_l = \sigma_r = 0$, like in the original RA-STM method, and two exact variables, T & θ , obtained from experiment. Therefore, the proposed method results in an exact solution.

Table 2.2 Comparison with the original RA-STM and the proposed method

Model	No. of Variables	No. of Equations	Differences	Given	Solving Method
Original RA-STM	19	16	3	$\sigma_l = \sigma_r = 0$ (or $\sigma_l = \text{cont.}$) $\varepsilon_d = \text{variable}$	Iterative
Proposed Method	17	13	4	$\sigma_l = \sigma_r = 0$ (or $\sigma_l = \text{cont.}$) Experimental T & θ	Exact Solution

2.3 Thickness of Shear Flow Zone

The thickness of shear flow zone, t_d , can be expressed as an equation of fourth degree in terms of known values, ε_d , ε_r , T and θ and throughout the combination of Eqn. 2.3, 2.4, 2.7 and 2.8.

$$(D - t_d)^3 t_d - \frac{8T}{\pi\theta} \left(\frac{-\varepsilon_d + \varepsilon_r}{-\sigma_d + \sigma_r} \right) = 0 \quad (2.18)$$

where D = Diameter of circular column

Another expression for t_d can be derived by substituting the steel ratios, ρ_l and ρ_r into Eqn. 2.1 and 2.2. The resulting equation gives

$$t_d = \frac{A_s f_l / p_o + A_t f_t / s}{\sigma_l + \sigma_r - \sigma_d - \sigma_r} \quad (2.19)$$

where

$$\rho_l = \frac{A_s}{p_o t_d}, \quad \rho_r = \frac{A_t}{s t_d} \quad (2.20)$$

Both of equations are used as a necessary condition during the calculation. As a result, exact solutions of t_d can be obtained from Eqn. 2.18, and then proved through Eqn. 2.19. By using this value, additional variables needed for torsion problem, A_0 and p_0 , which are cross-sectional area and perimeter bounded by the centerline of the shear flow zone respectively are calculated according to Eqn. 2.21 and 2.22.

$$A_0 = A_c - \frac{1}{2} p_c t_d + t_d^2 \quad (2.21)$$

$$p_0 = p_c - 4t_d \quad (2.22)$$

3. CONSTITUTIVE RELATIONSHIPS OF MATERIALS

3.1 Constitutive Relationships under Biaxial Loading

The stress-strain relationships of concrete and steel are based on the set of biaxial strains. The set of biaxial stresses cannot be calculated directly from the biaxial strains using the biaxial constitutive relationships. Because these relationships depend on the Poisson effect and cannot be uniquely established from test. Therefore, it is necessary to connect the biaxial stresses to biaxial strains ($\varepsilon_1, \varepsilon_2$) containing the set of uniaxial strains ($\bar{\varepsilon}_1, \bar{\varepsilon}_2$). Hsu and Zhu (2002) derived these relations from their panel tests and suggested following equations.

$$\bar{\varepsilon}_1 = \frac{1}{1 - \nu_{12}\nu_{21}} \varepsilon_1 + \frac{\nu_{12}}{1 - \nu_{12}\nu_{21}} \varepsilon_2 = \varepsilon_1 + \nu_{12}\varepsilon_2 \quad (3.1)$$

$$\bar{\varepsilon}_2 = \frac{\nu_{21}}{1 - \nu_{12}\nu_{21}} \varepsilon_1 + \frac{1}{1 - \nu_{12}\nu_{21}} \varepsilon_2 = \varepsilon_2 \quad (3.2)$$

$$\bar{\varepsilon}_l = \varepsilon_2 \cos^2 \alpha + (\varepsilon_1 + \nu_{12}\varepsilon_2) \sin^2 \alpha \quad (3.3)$$

$$\bar{\varepsilon}_t = \varepsilon_2 \sin^2 \alpha + (\varepsilon_1 + \nu_{12}\varepsilon_2) \cos^2 \alpha \quad (3.4)$$

where

$$\nu_{12} = 0.2 + 850\varepsilon_{sf}, \quad \varepsilon_{sf} \leq \varepsilon_y \quad (3.5a)$$

$$\nu_{12} = 1.9, \quad \varepsilon_{sf} > \varepsilon_y \quad (3.5b)$$

$$\nu_{21} = 0 \quad (3.6)$$

3.2 Constitutive Relationships under Uniaxial Loading

The uniaxial constitutive relationships of the concrete and steel bars are given below, with the emphasis on improvements. The relationship between σ_d and $\bar{\varepsilon}_d$ is assumed to be parabolic. The constant 4 in the descending-branch of equation Eqn. (3.7b) replaces the old constant 2 (Pang and Hsu 1996). This revision is intended to take care of a long plateau after the peak-point that was observed in the strain-controlled tests.

$$\sigma_d = \zeta f_c \left[2 \left(\frac{\bar{\varepsilon}_d}{\zeta \varepsilon_0} \right) - \left(\frac{\bar{\varepsilon}_d}{\zeta \varepsilon_0} \right)^2 \right]; \quad \text{when } \left(\frac{\bar{\varepsilon}_d}{\zeta \varepsilon_0} \right) \leq 1 \quad (3.7a)$$

$$\sigma_d = \zeta f_c \left[1 - \left(\frac{\bar{\varepsilon}_d / \zeta \varepsilon_0 - 1}{4 / \zeta - 1} \right)^2 \right]; \quad \text{when } \left(\frac{\bar{\varepsilon}_d}{\zeta \varepsilon_0} \right) \geq 1 \quad (3.7b)$$

$$\zeta = \frac{5.8}{\sqrt{f_c} (Mpa)} \frac{1}{\sqrt{1 + 400\bar{\varepsilon}_r}} \leq 0.9 \quad (3.8)$$

To account for the tension stiffening effect, an average tensile stress-strain relationship of concrete proposed by Greene (2006) was chosen as shown in Eqn 3.9(a) and (b).

$$\sigma_r = E_c \bar{\varepsilon}_r; \quad \text{when } \bar{\varepsilon}_r \leq \varepsilon_{cr} \quad (3.9a)$$

$$\sigma_r = f_{cr} e^{-379.6(\bar{\varepsilon}_r - \varepsilon_{cr})}; \quad \text{when } \bar{\varepsilon}_r > \varepsilon_{cr} \quad (3.9b)$$

The relationship of f_s and $\bar{\varepsilon}_s$ is expressed by a bilinear model. In Eqn. (3.10), l replaces s in the subscripts of the symbols for longitudinal steel, and t replaces s in the subscripts of the symbols for transverse steel.

$$f_s = E_s \bar{\varepsilon}_s; \quad \text{when } \bar{\varepsilon}_s \leq \bar{\varepsilon}_n \quad (3.10a)$$

$$f_s = f_y [(0.91 - 2B) + (0.02 + 0.25B) \frac{\bar{\varepsilon}_s}{\varepsilon_y}] \quad \text{when } \bar{\varepsilon}_s > \bar{\varepsilon}_n \quad (3.10b)$$

where

$$\bar{\varepsilon}_n = \varepsilon_y (0.93 - 2B), \quad B = \frac{1}{\rho} \left(\frac{f_{cr}}{f_y} \right)^{1.5}$$

4. MODIFIED ALGORITHM AND VALIDATION

4.1 Method of Solution

The following algorithm is used to solve the system of governing equations for a specific loading point on the whole torque-twist curve.

1. Given T & θ from experimental data
2. Assume t_d
3. Assume ε_r
4. Assume ε_d
5. Calculate A_0, p_0, ρ_t, ρ_l from Eqn. (2.21), (2.22) and (2.20)
6. Calculate γ_{lt} from Eqn. (2.8)
7. Calculate α from Eqn. (2.7)
8. Calculate $\varepsilon_l, \varepsilon_r$ from Eqn. (2.5) and (2.6)
9. Calculate v_{12} from Eqn. (3.5)
10. Calculate $\bar{\varepsilon}_d, \bar{\varepsilon}_r, \sigma_d$ and σ_r from Eqn. (3.1),(3.2),(3.7) and (3.9)
11. Calculate $\bar{\varepsilon}_l, \bar{\varepsilon}_r, f_l, f_t$ from Eqn (3.3),(3.4) and (3.10)
12. Is σ_l close from Eqn. (2.1)? Go to step 4
13. Is σ_r close from Eqn. (2.2)? Go to step 3
14. Is t_d close from Eqn. (2.18)? Go to step 2
15. Calculate $\tau_{lt}, \gamma_{lt}, T, \theta$ from Eqn. (2.3), (2.7), (2.4) and (2.8)
16. Check the given and calculated T, θ and t_d from Eqn. (2.19)

4.2 Calculated Results and Validation

Testing of half-scale circular RC column under torsion and axial force was carried out by Belarbi et al., (2008). The test results from this study were used for the calculation and validation of the proposed method. The torque versus twist hysteresis curve and the envelope under positive cycle of loading is shown in Figure 2 with the calculated points. Calculation using the proposed method was carried out based on this information and the results of the calculation are summarized in Table 4.1. Uni-axial and biaxial strains of transverse and longitudinal reinforcement calculated from the proposed method are compared with experimental strains located at the middle of length column not affected by boundary condition. The behavior of the column is predominated by the transverse reinforcement under pure torsion due to relatively lower ρ_t than ρ_l . This makes transverse reinforcement to yield before the peak-point (at which concrete reaches its peak value) while longitudinal reinforcement yields thereafter. Hus/Zhu's Poisson ratios are also determined according to the behavior of the transverse steel. Experimental strains in transverse reinforcement differ from the proposed method depending on their location near the crack as shown in Figure 3(a). Two of them decrease slightly with respect to torque after the peak point with the small increase of strain, while the other decreases with large increase of strain. However, all of experimental and analytical curves show that they yield before the peak point.

The analytical results were in reasonable agreement with the experimental ones using the adopted average strain concept. Even after yielding of spiral, experimental and calculated strain values slightly increase with torque and this is due to fact that bars are stiffened by surrounded concrete until the peak point. It is clear that use of average stress-strain concept for steel adopted in the proposed method is effective from this point of view. After the peak point, all curves start to decrease with respect to torque for maintaining the equilibrium condition. Both of uni- and bi-axial strain curves increase after the peak point, because they already exceed the yielding point. It is also apparent that biaxial strain is higher than uniaxial strain due to the inclusion of Poisson's effect. Experimental strain

values of longitudinal reinforcement also show difference in behavior compared to analytical prediction as observed in strains of transverse reinforcement shown Figure 3(b). The calculated uniaxial strain curves in longitudinal steel show a good agreement with the experimental results in terms of strain values. However, predictions of strain using the proposed method show a difference in trend as observed in transverse steel. After the peak point, biaxial strain curve significantly increases in terms of strain value, while uniaxial strain curves decreases, because the longitudinal steel has not yielded even after the peak point. As a result, longitudinal bar takes most part of internal forces after the peak point. Adoption of Poisson's effect in the proposed method can provide a rational estimation after the peak point.

Table 4.1 Example of Iteration and Calculated results by the proposed method

STEP	1	2	3	4	5	6	7
T	136	181	203	209	264	278	243
θ	0.000267	0.000527	0.0001611	0.0002021	0.0004426	0.0011469	0.0020376
ε_d	-0.00013	-0.00016	-0.00022	-0.00026	-0.00041	-0.00107	-0.00306
ε_r	0.000145	0.000361	0.001382	0.001805	0.004175	0.011834	0.018348
t_d	14.95	18.73	19.60	17.76	18.30	20.46	21.66
ε_t	0.000040	0.000161	0.000816	0.001083	0.002703	0.008929	0.012724
ε_l	-0.000027	0.000038	0.000343	0.000464	0.001060	0.001831	0.002559
ν_{12}	0.23	0.34	0.89	1.12	1.90	1.90	1.90
$\bar{\varepsilon}_r$	0.000021	0.000128	0.000688	0.000895	0.002171	0.007347	0.008431
$\bar{\varepsilon}_l$	-0.000039	0.000017	0.000273	0.000362	0.000809	0.001372	0.001030
$\bar{\varepsilon}_r$	0.000114	0.000306	0.001183	0.001516	0.003392	0.009793	0.012525
ζ	0.88	0.85	0.74	0.71	0.59	0.41	0.37
σ_d	-4.40	-5.30	-7.08	-8.10	-11.70	-13.96	-11.35
σ_r	2.62	2.91	2.09	1.84	0.90	0.08	0.03
\bar{f}_l	-8.03	3.52	56.45	74.92	167.15	283.51	212.81
\bar{f}_l	4.26	26.40	142.18	184.90	365.19	400.37	407.01
α	38.04	38.16	36.42	36.27	34.51	28.32	30.83
γ_{lt}	0.000270	0.000508	0.001532	0.001969	0.004283	0.010782	0.018846
θ	0.000027	0.000053	0.000161	0.000202	0.000443	0.001147	0.002038
T	136	181	203	209	264	278	243

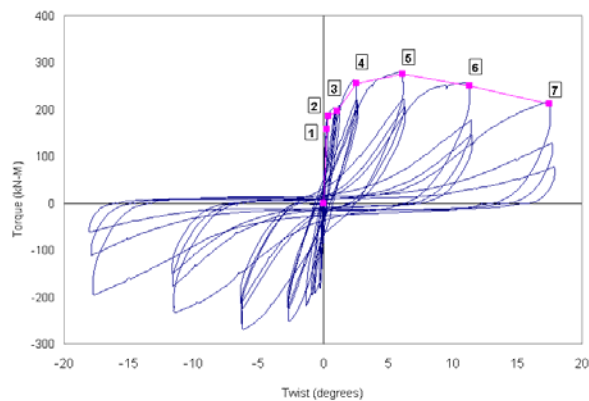


Figure 2 Torque-twist response

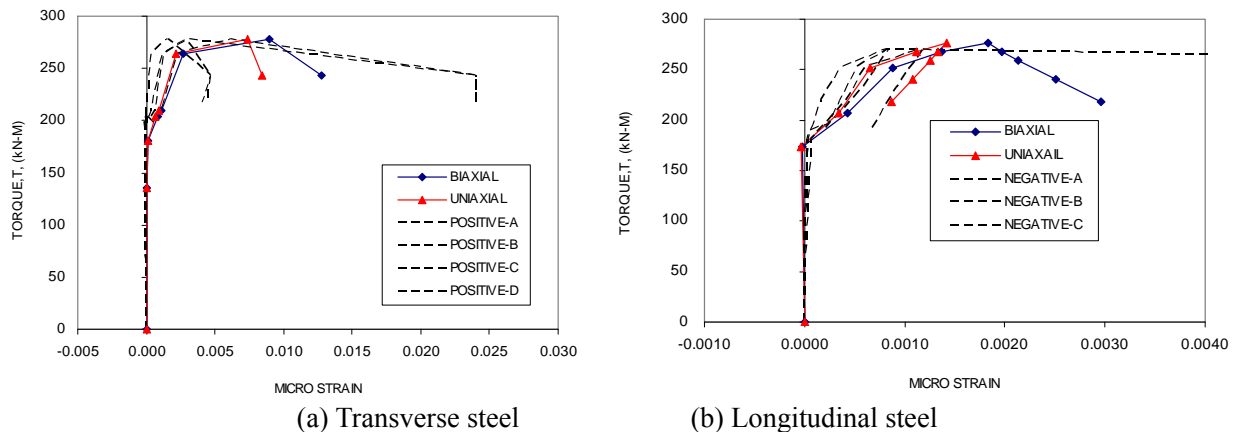


Figure 4 Torque versus uni-axial and biaxial strains in reinforcement

5. CONCLUSIONS

An analytical model to predict the behavior of circular RC column subjected to torsion and axial force was proposed. The proposed model not only includes the tension stiffening effect of concrete to provide a continuous prediction before and after cracking but also the Poisson effect. This makes it possible to predict the behavior after post-peak without any difficulties that are associated with not satisfying the equilibrium conditions at the peak-point. In addition, the thickness of shear flow zone, t_d , is properly estimated by using a rational equilibrium equation. The estimation method for t_d is totally different between the rectangular and circular section due to out-of-plane warping effect to concrete struts. This particular feature of the proposed model will play role not only as a good basis for the further development of analytical model for the circular RC columns under combined loading but also as a verification tool for a rectangular member under pure torsion.

REFERENCES

- Belarbi, A. and Hsu, T.T.C. (1994). Constitutive laws of concrete in tension and reinforcing bars stiffened by concrete. *ACI Structural Journal*, **91:4**, 465-474.
- Belarbi, A. and Hsu, T.T.C. (1995) Constitutive laws of softened concrete in biaxial tension-compression. *ACI Structural Journal*, **92: 5**, 562-573.
- Belarbi, A, Suriya Prakash, S. and Ayoub, A. (2008). An experimental study on behavior of RC bridge columns under combined cyclic bending and torsion. *Concrete Bridge Conference*, St Louis, Missouri, USA May 5-7. Paper No. 5.
- Greene, G.G. (2006). Behavior of RC girders under cyclic torsion and torsion combined with shear: experimental investigation and analytical models. *Ph.D. thesis, Department of Civil, Architectural, and Environmental Engineering, University of Missouri at Rolla*, 227.
- Hsu, T.T.C. (1988). Softened truss model theory for shear and torsion. *ACI Structural Journal*, **85:6**, 624-635.
- Hsu, T.T.C. and Zhang, L.X. (1997). Nonlinear analysis of membrane elements by fixed-angle softened truss model. *ACI Structural Journal*, **94:5**, 483-492.
- Hsu, T.T.C. (1998). Stresses and crack angles in concrete membrane elements. *Journal of Structural Engineering* **124:12**, 1476-1484.
- Hsu, T. T. C. and Zhu, R.R.H. (2002a). Softened membrane model for reinforced concrete elements in shear. *ACI Structural Journal* **99:4**, 460-469.
- Hsu, T. T. C. and Zhu, R. R.H. (2002b). Poisson effect in reinforced concrete membrane elements. *ACI Structural Journal* **99:5**, 631-640.
- Pang, X.B. and Hsu, T.T.C. (1996). Fixed-angle softened truss model for reinforced concrete. *ACI Structural Journal* **93:2**, 197-207.
- Sengupta, A.K. and Belarbi, A. (2001). Modeling effect of biaxial stresses on average stress-strain relationship of reinforcing bar in reinforced concrete panels. *ACI Structural Journal*, **98:5**, 629-637.
- Vecchio, F.J. and Collins, M.P. (1986). The modified compression field theory for reinforced concrete element subjected to shear. *ACI Structural Journal*, **83:2**, 219-231.